2-(*N*-morpholino)-ethanesulfonic acid (MES)–KOH (pH 6.1), 15 μM PLP], whereas all other data were collected from crystals soaked in stabilization buffer [buffer B: 20% PEG4000, 100 mM sodium pyruvate, 30 mM MES-NaOH (pH 6.1), 20 μM PLP]. All derivatives were isomorphous only with the native B data. The major heavy atom binding sites were found with vector searches of difference Patterson maps by standard CCP4 programs [CCP4, *SERC U.K. Collaborative Computing Project No. 4* (Daresbury Laboratory, United Kingdom, 1979)]. Heavy atom parameters were refined against the centric data and multiple isomorphous replacement (MIR) phases were calculated. The 2.8 Å MIR map was improved with several cycles of solvent flattening [B.-C. Wang, *Methods Enzymol.* **115**, 90 (1985)]. A model containing 88% of the atoms was built with the program O [T. A. Jones and M. Kjelgaard, *Manual for O* (Uppsala University, Uppsala, Sweden, 1990)] into a map flattened at 45% solvent content and was refined with X-PLOR [A. T. Brünger, *X-PLOR Manual* (Yale Univ. Press, New Haven, CT, 1990)] and a simulated annealing protocol. Combination of MIR and partial model phases and additional solvent flattening resulted in a map that allowed the entire sequence to be traced. A second application of simulated annealing at 2.8 Å resolution was performed. The native A structure was obtained by direct refinement of the native B model against native A data with an X-PLOR simulated annealing protocol. Thereafter, refinement proceeded with the program TNT [D. E. Tronrud, L. F. Ten Eyck, B. W. Matthews, *Acta. Crystallogr. Sect. A* **43**, 489 (1987)] with all observed data between 8 Å and the respective high-resolution limits.

4. J. N. Jansonius and M. G. Vincent, in *Biological Macromolecules and Assemblies*, F. A. Jurnak and A. McPherson, Eds. (Wiley-Interscience, New York, 1987), vol. 3, pp. 187–286; C. A. McPhalen, M. G. Vincent, J. N. Jansonius, *J. Mol. Biol.* **225**, 495 (1992); G. C. Ford, G. Eichele, J. N. Jansonius, *Proc. Natl. Acad. Sci. U.S.A.* **77**, 2559 (1980).
5. N. Watanabe *et al.*, *J. Biochem.* (*Tokyo*) **105**, 1 (1989).
6. A. A. Antson *et al.*, *Biochemistry* **32**, 4195 (1993).
7. H. C. Dunathan, *Proc. Natl. Acad. Sci. U.S.A.* **55**, 712 (1966).
8. External aldimine models were built on minimal assumptions and manipulations of the enzyme structure. The coenzyme ring in the aldimine models is rotated forward (in the view of Fig. 2) compared with the holoenzyme to relieve steric clashes. By analogy to AAT (*4*), this rotation was achieved by a change in only the C4-C5-C5′-OP1 torsion angle of PLP (64° to 91°). The indole ring of Trp^{138} rotates to near planarity with the PLP ring to accommodate the change in coenzyme conformation.
9. T. Gallagher, E. E. Snell, M. L. Hackert, *J. Biol. Chem.* **264**, 12737 (1989).
10. M. H. O'Leary, *Acc. Chem. Res.* **21**, 450 (1988); J. F. Marlier and M. H. O'Leary, *J. Am. Chem. Soc.* **108**, 4896 (1986); J. A. Ashley *et al.*, *ibid.* **115**, 2515 (1993).
11. M. D. Toney and J. F. Kirsch, *Science* **243**, 1485 (1989); *Biochemistry* **32**, 1471 (1993).
12. DGD crystals were dissolved, the protein was hydrolyzed (10 M hydrochloric acid, 90°C, 1.5 hours), and the Ca^{2+} content was determined fluorometrically [J. P. Y. Kao, A. T. Harootunian, R. Y. Tsien, *J. Biol. Chem.* **264**, 8179 (1989)] to be less than 0.2 and 0.1 Ca^{2+} per DGD monomer in native A and B, respectively. The Ca^{2+} concentrations in the buffers are 10 to 30 μM.
13. In native A, the *B* factor for a K^+ ion at site 1 refined with full occupancy is 13 $Å^2$, compared with an average ligand value of 19 $Å^2$. Refinement of Na^+, or Ca^{2+} with partial occupancy, results in very low metal *B* factors and strong, positive difference electron density centered on the metal ion. Refinement of K^+ with full occupancy at site 2 in native A gives a *B* factor (47 $Å^2$) that is significantly higher than the average ligand value (19 $Å^2$). In contrast, Na^+ with full occupancy at site 2 yields a *B* factor of 26 $Å^2$ compared with an average ligand value of 19 $Å^2$. In native B, Na^+ refined with full occupancy at site 1 has a *B* factor of 31 $Å^2$ compared with an average ligand value of 24 $Å^2$. At site 2, Na^+ refined with full occupancy has a *B* factor of 31 $Å^2$ compared with an average ligand value of 27 $Å^2$. Refinement of several alternative native B models with partial occupancies for K^+ or Ca^{2+} invariably yielded either *B* factors significantly different from the average ligand values or strong residual difference density centered on the metal ion, or both.
14. Standard metal-oxygen distances are 2.1 Å for Mg^{2+}, 2.4 Å for Na^+ and Ca^{2+}, and 2.7 to 2.8 Å for K^+ [J. P. Glusker, *Adv. Protein Chem.* **42**, 1 (1991); C. A. McPhalen, N. C. J. Strydnadka, M. N. G. James, *ibid.*, p. 77; M. M. Yamashita, L. Wesson, G. Eisenman, D. Eisenberg, *Proc. Natl. Acad. Sci. U.S.A.* **87**, 5648 (1990)]. The average metal-ligand distances obtained for the metals assigned to the final models are 2.73 and 2.33 Å at site 1 and 2.39 and 2.42 Å at site 2 in native A and native B, respectively. Metal-ligand distances were completely unrestrained during the refinement procedures, and no electrostatic or van der Waals energy terms were used.
15. DGD requires K^+ ions for activity and stability, whereas Li^+ and Na^+ are inhibitory [H. G. Aaslestad, P. J. Bouis, Jr., A. T. Philips, A. D. Larson, in *Pyridoxal Catalysis: Enzymes and Model Systems*, E. E. Snell, A. E. Braunstein, E. S. Severin, Y. M. Torchinsky, Eds. (Wiley-Interscience, New York, 1968), pp. 479–490].
16. G. Eisenman and J. A. Dani, *Annu. Rev. Biophys. Biophys. Chem.* **16**, 205 (1987); M. Dobler, *Ionophores and Their Structures* (Wiley, New York, 1981); R. M. Izatt *et al.*, *Chem. Rev.* **85**, 271 (1985); F. Vögtle and E. Weber, Eds., *Host Guest Complex Chemistry: Macrocycles* (Springer, Berlin, 1985); D. Cram, *Angew. Chem. Int. Ed. Engl.* **25**, 1039 (1986).
17. C. H. Suelter, *Science* **168**, 789 (1970). Nonspecific binding of Na^+ and K^+ ions to proteins has been observed crystallographically with subtilisin BPN′ [M. W. Pantoliano *et al.*, *Biochemistry* **27**, 8311 (1988)], thermitase [P. Gros *et al.*, *J. Mol. Biol.* **210**, 347 (1989)], and insulin [O. Gursky, Y. Li, J. Badger, D. L. D. Caspar, *Biophys. J.* **61**, 604 (1992)]. Crystallographic observation of the essential K^+ ion in pyruvate kinase has remained elusive [H. Muirhead, in *Biological Macromolecules and Assemblies*, F. A. Jurnak and A. McPherson, Eds. (Wiley-Interscience, New York, 1987), vol. 3, pp. 143–186].
18. M. Carson, *J. Mol. Graph.* **5**, 103 (1987).
19. We thank J. W. Keller for supplying the enzyme, P. Maurer for performing the calcium determination experiments, and U. Sauder for providing expert technical assistance. Supported by Swiss National Science Foundation grant 31-25712.88 (J.N.J.) and by U.S. National Institutes of Health fellowship GM13854 (M.D.T.).

16 March 1993; accepted 25 June 1993

DNA Melting on Yeast RNA Polymerase II Promoters

Charles Giardina and John T. Lis*

Transcription-dependent DNA melting on the yeast *GAL1* and *GAL10* promoters was found to be more closely correlated with the TATA box than the transcription start site. On both these genes, melting begins about 20 base pairs downstream of the TATA box. Physical and genetic analyses suggest that RNA polymerase II associates with this region. Thus, the distance between promoter melting and the TATA box in yeast may be similar to that in higher eukaryotes, even though transcription initiates in a region about 10 to 90 base pairs farther downstream in yeast.

In prokaryotes, the melting of the DNA helix at the commencement of transcription often requires only the RNA polymerase and promoter sequence elements (*1*). For eukaryotic RNA polymerase II genes, this melting reaction also depends on RNA polymerase II but in addition requires basal transcription factors and adenosine triphosphate (ATP) hydrolysis (*2*). On TATA-containing promoters, the transcription factor TFIID first associates with the TATA box followed by the other basal factors and polymerase (*3*). After this assembly, the DNA can be melted in an ATP-dependent reaction, with residues approximately 12 base pairs (bp) upstream through 3 bp downstream of the transcriptional start site being unwound to form an open complex (*4*, *5*).

In higher eukaryotes, the locations of promoter melting and transcription initiation overlap at ~30 bp from the TATA box (*4–6*). In yeast the distance between the location of the transcriptional startsite and the TATA box is highly variable, ranging from 30 to 120 bp (*7*). This is true even though the basal transcription factors and the polymerase are highly conserved between yeast and higher eukaryotes (*8–12*). We wanted to determine, therefore, how promoter melting in yeast is positioned relative to the start site and the TATA box. We used the DNA modifying reagent potassium permanganate ($KMnO_4$) which reacts preferentially with T residues in single-stranded DNA (*13*). Although open polymerase complexes can be difficult to detect under steady-state conditions, $KMnO_4$ hyperreactivity of these complexes can be detected on some promoters in *Escherichia coli* (*14*). We have also detected what appear to be open polymerase complexes in *Drosophila* cells in vivo, suggesting that these complexes have a dwell time long enough to allow their detection in eukaryotes (*15*).

Section of Biochemistry, Molecular, and Cell Biology, Cornell University, Ithaca, NY 14853.

*To whom correspondence should be addressed.

The first gene we analyzed was *GAL1* because it is highly inducible; addition of galactose to the media (in the absence of glucose) gives about a 1000-fold induction of *GAL1* transcription (*16*). The $KMnO_4$ modification pattern on the *GAL1* gene is shown for cells grown with glucose, raffinose (another noninducing sugar), or galactose as the carbon source (Fig. 1). The pattern of $KMnO_4$ reactivity of purified yeast genomic DNA is also shown. When compared with the $KMnO_4$ modification pattern on the uninduced *GAL1* gene and on purified DNA, the *GAL1* gene in cells grown in galactose was $KMnO_4$ hyperreactive from the transcriptional start site to 66 bp upstream (*17*). Every T residue on both strands of DNA, from the −66 position (relative to the major transcriptional start site) through the transcriptional start site, displayed some degree of hyperreactivity (see Fig. 2 for compiled results) (*18*). The characteristics of this $KMnO_4$ hyperreactivity are consistent with extensive melting of the DNA helix upstream of the transcriptional start site. The 5′ end of this DNA melting we observed on the *GAL1* gene is at a distance from the TATA box similar to that of an open complex of a higher eukaryote (~20 bp) (*4, 5, 15*). It is possible that polymerase associates with the *GAL1* gene and melts the DNA at a location determined by the TATA box.

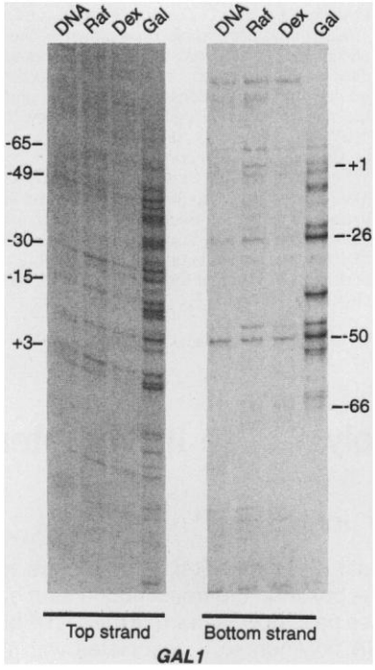

Fig. 1. The $KMnO_4$ reactivity of the *GAL1* gene in vivo at different states of activation. Cells were grown in rich media with raffinose (Raf), dextrose (Dex), or galactose (Gal), as indicated. A logarithmically growing culture was treated for 1 min with 25 mM $KMnO_4$ at 22°C. Also shown is purified genomic DNA treated with 25 mM $KMnO_4$ for 30 s at 22°C. The DNA was then purified and cleaved at the modification sites with piperidine. The sites of cleavage were viewed by the ligation-mediated polymerase chain reaction (LMPCR), with the use of primers to display either the top (coding) or bottom (transcribed) DNA strand, as indicated (*25*). The numbers at the sides of the gels indicate positions relative to the major *GAL1* transcriptional startsite (*17*).

To study the influences of the TATA box and the transcriptional start site on promoter DNA melting, we mapped the $KMnO_4$ hyperreactivity on the induced *GAL10* gene. The TATA box on the *GAL10* gene is 114 bp from the major transcriptional start site compared with the 84-bp distance on the *GAL1* gene (*17*). If promoter DNA melting is directed by the TATA box, the region of melting on the *GAL10* gene should extend farther upstream from the transcriptional start site than it does on the *GAL1* gene. Induction of the *GAL10* gene by growth on galactose produced a region of melted DNA extending ~92 bp upstream of the transcriptional start site compared with the ~66 bp of melting upstream of the *GAL1* start site (Fig. 3). The 5′ end of this melted region is again similar to that of an open complex of a higher eukaryote (see Fig. 2 for compiled results).

The $KMnO_4$ hyperreactivity in the region between the *GAL10* TATA box and transcriptional start site was uneven; both strands were more hyperreactive at the 5′ portion of this melted region (the −92 through −34 region). It is possible that polymerase density is higher over the −92 through −34 region than over the −33 through −1 region. This effect was not observed on the *GAL1* gene, perhaps because the distance between the TATA box and the start site is shorter.

The DNA melting we observed could

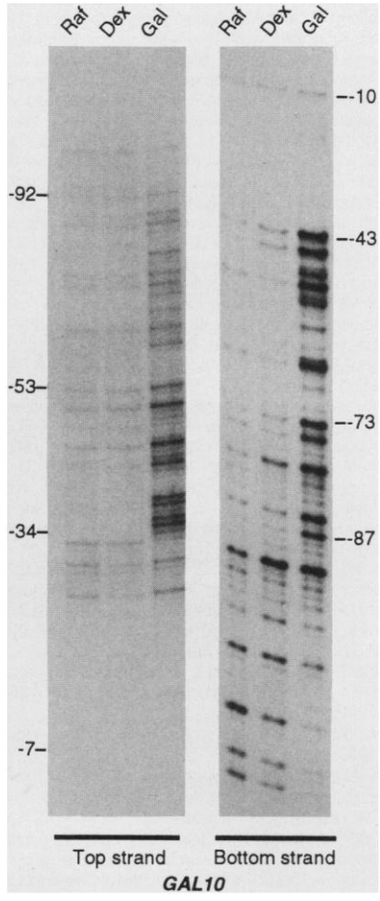

Fig. 3. The $KMnO_4$ reactivity of the *GAL10* gene in vivo at different states of activation. Cells were grown in rich media with raffinose (Raf), dextrose (Dex), or galactose (Gal), as indicated. Treatment with $KMnO_4$ and subsequent processing to view the $KMnO_4$ modification sites were performed as described (Fig. 1). The left panel shows the results for the top DNA strand, and the right panel, for the bottom strand (*26*). The numbers at the sides of the gels indicate positions relative to the major *GAL10* transcriptional start site (*17*).

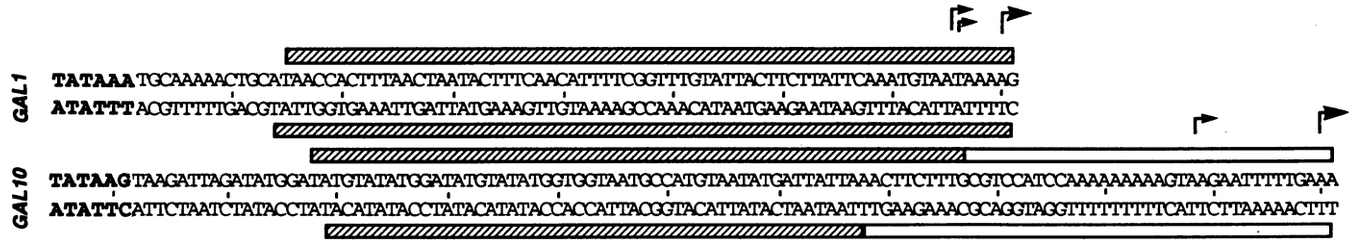

Fig. 2. The extent of $KMnO_4$ hyperreactivity on the *GAL1* and *GAL10* genes after transcriptional activation. For the *GAL10* gene, striped bars indicate $KMnO_4$ hyperreactive regions and open bars represent regions of lower hyperreactivity. The TATA boxes are shown in bold print. The major transcriptional start site on each gene is indicated by the large arrow, with minor upstream sites indicated by smaller arrows (*17*).

have been the result of a structure like an open polymerase complex; however, we also considered the possibility that the melting might be the result of negative supercoiling, which would be expected to form transiently in the wake of transcribing polymerases (*19*). Melting induced by negative supercoiling can be reversed by lowering the temperature, whereas melting in an open complex is often stable at low temperatures (*20–22*). Temperature- and supercoil-dependent melting of the *GAL1* promoter in purified DNA is shown (Fig. 4A). Raising the temperature from 22° to 45°C increases $KMnO_4$ reactivity at a number of sites. This temperature-dependent increase in reactivity depends on DNA supercoiling because such an effect is not observed on a linear molecule. Comparing the $KMnO_4$ hyperreactivity on the *GAL1* gene in vivo at 22°C with that at 0°C shows that the melting in vivo is not affected by lowering the temperature (Fig. 4B). This melting, therefore, appears to be stabilized, possibly by RNA polymerase II.

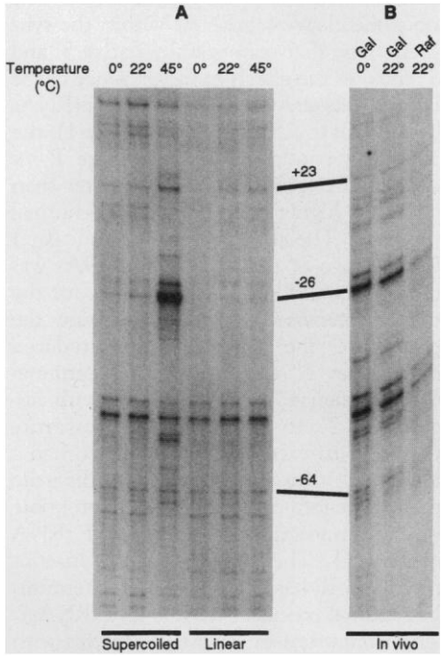

Fig. 4. (**A**) Supercoil- and temperature-dependent $KMnO_4$ hyperreactivity of the *GAL1* promoter in vitro. We treated supercoiled or linear (restriction cut) plasmid with 25 mM $KMnO_4$ for 30 s at the temperatures shown (*27*). Modification sites were cleaved with piperidine and viewed by LMPCR. The numbers at the side of the gel indicate positions relative to the major *GAL1* transcriptional start site (*17*). (**B**) The $KMnO_4$ reactivity of the *GAL1* promoter in vivo at 0° and 22°C. Cells were grown at 30°C to logarithmic phase in galactose (Gal) or raffinose (Raf), centrifuged, and resuspended in 0° or 22°C media (as indicated) for treatment with 25 mM $KMnO_4$ for 1 min. We processed DNA as described (Fig. 1) to view the $KMnO_4$ modification sites.

To obtain additional evidence that the DNA melting upstream of the transcriptional start site was the result of RNA polymerase II, we analyzed the $KMnO_4$ reactivity pattern on the *GAL1* gene in an *rpb1-1* yeast strain. The *rpb1-1* mutation is a tight temperature-sensitive mutation in the largest subunit of RNA polymerase II. Raising the temperature from 24° to 36°C selectively inactivates RNA polymerase II transcription in this strain (*23*). When cells were at 24°C, there was little difference in the $KMnO_4$ reactivity pattern of the *GAL1* gene in yeast with the wild-type or *rpb1-1* allele (Fig. 5). However, shifting the temperature to 36°C inhibited DNA melting of the *GAL1* promoter in the *rpb1-1*–carrying strain but had little effect on the wild-type strain. The extensive region of melting upstream of the *GAL1* transcriptional start site is therefore dependent on the activity of RNA polymerase II.

If the DNA melting upstream of the transcriptional start site is the result of polymerase association with this region, it is unlikely that polymerase initiates transcription ~30 bp downstream from the TATA box, with a mature 5′ end being formed by cleavage of the RNA. Lue *et al.* (*24*) were able to synthesize properly initiated RNAs in the presence of a chain-terminating nucleotide that would have prevented transcription from 30 bp downstream of the TATA to the cap site. We hypothesize that polymerase associates with the promoter, melts the DNA, and locates the start site by scanning the DNA.

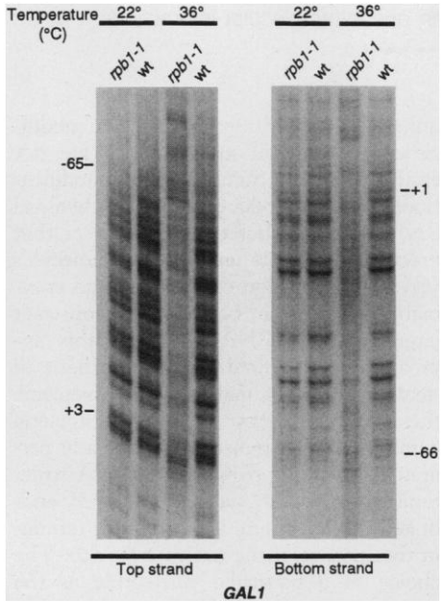

Fig. 5. Inhibition of *GAL1* promoter melting in a temperature-sensitive RNA polymerase II strain. The $KMnO_4$ hyperreactivity of *GAL1* was analyzed in yeast strains carrying either the wild-type (wt) or *rpb1-1* temperature-sensitive allele of the *RPB1* gene. Cells were grown in galactose media at 24°C and either shifted to 36°C for 10 min before $KMnO_4$ treatment (also done at 36°C) or treated at 22°C. We then prepared DNA and processed it as described (Fig. 1).

Although the promoter melting we observed is dependent on polymerase activity, the possibility remains that polymerase does not associate directly with this region of the gene. For example, negative supercoiling generated by transcribing polymerases could be trapped by a protein that binds single-stranded DNA, or a transcription factor might melt this portion of the promoter with the aid of polymerase. Whether or not the region of melting upstream of the start site is the result of polymerase entry, its location raises some interesting possibilities.

REFERENCES AND NOTES

1. P. H. vonHippel, D. G. Bear, W. D. Morgan, J. A. McSwiggen, *Annu. Rev. Biochem.* **53**, 389 (1984).
2. W. Wang *et al.*, *Genes Dev.* **6**, 1716 (1992).
3. L. Zawel and D. Reinberg, *Curr. Opin. Cell Biol.* **4**, 488 (1992).
4. S. Buratowski *et al.*, *Proc. Natl. Acad. Sci. U.S.A.* **88**, 7509 (1991).
5. W. Wang, M. Carey, J. D. Gralla, *Science* **255**, 450 (1992).
6. J. Corden *et al.*, *ibid.* **209**, 1406 (1980).
7. K. Struhl, *Cell* **49**, 295 (1987).
8. B. Cavallini *et al.*, *Proc. Natl. Acad. Sci. U.S.A.* **86**, 9803 (1989).
9. O. Gileadi, W. J. Feaver, R. D. Kornberg, *Science* **257**, 1389 (1992).
10. J. A. Ranish, W. S. Lane, S. Hahn, *ibid.* **255**, 1127 (1992).
11. R. A. Young, *Annu. Rev. Biochem.* **60**, 689 (1991).
12. I. Pinto *et al.*, *Cell* **68**, 977 (1992).
13. C. M. Rubin and C. W. Schmid, *Nucleic Acids Res.* **8**, 4613 (1980).
14. S. Sasse-Dwight and J. D. Gralla, *J. Biol. Chem.* **264**, 8074 (1989).
15. C. Giardina, M. Perez-Riba, J. T. Lis, *Genes Dev.* **6**, 2190 (1992).
16. T. P. St. John and R. W. Davis, *J. Mol. Biol.* **152**, 285 (1981).
17. M. Johnston and R. W. Davis, *Mol. Cell. Biol.* **4**, 1440 (1984).
18. The $KMnO_4$ hyperreactivity observed here is less than that observed for trapped open polymerase complexes probed with $KMnO_4$ in *E. coli*, where such complexes are probably formed on almost all the genes being analyzed (*14*). Therefore, it is possible that the melting we observed occurred on only a fraction of the genes being assayed. This observation is consistent with the melted DNA complexes being formed transiently in vivo. It should also be noted that weaker $KMnO_4$ hyperreactivity was evident downstream of the transcriptional start site. We have observed a similar effect on actively transcribing genes in *Drosophila*, and it is presumably the result of DNA melting that is associated with elongating polymerase molecules (*15*).
19. L. F. Liu and J. C. Wang, *Proc. Natl. Acad. Sci. U.S.A.* **84**, 7024 (1987).
20. F. Aboul-ela, R. P. Bowater, D. M. J. Lilley, *J. Biol. Chem.* **267**, 1776 (1992).
21. E. Grimes, S. Busby, S. Minchin, *Nucleic Acids Res.* **19**, 6113 (1991).
22. W. Suh *et al.*, *Science* **259**, 358 (1993).
23. M. Nonet, C. Scafe, J. Sexton, R. Young, *Mol. Cell. Biol.* **7**, 1602 (1987).
24. N. F. Lue *et al.*, *Science* **246**, 661 (1989).
25. Ten milliliters of a logarithmic-phase culture grown in YEP (yeast extract with peptone) media

with dextrose, raffinose, or galactose was centrifuged and resuspended in 50 μl of the used media. We then treated this suspension with 3.5 μl of 0.35 M $KMnO_4$ for 1 min at 22°C. The reaction was stopped by dilution in sorbitol stop buffer [0.9 M sorbitol, 0.1 M tris-HCl (pH 8.0), 0.1 M EDTA, 40 mM β-mercaptoethanol]. Spheroplast preparation and DNA isolation was performed as described (*28*). Piperidine treatment and ligation-mediated polymerase chain reaction (LMPCR) analyses were performed as described (*15*). The primers used for LMPCR were the following: top strand, primer 1: GCGATTAGTTTTTTAGCCTTATTTCTGG; primer 2: TCTGGGGTAATTAATCAGCGAAGCGATG; and bottom strand, primer 1: CCAATGGTCTTGGTAATTCCTTTGC; primer 2: TTTGCGCTAGAATTGAACTCAGGTAC.

26. The primers used for LMPCR were the following: top strand, primer 1: ATTAGCTCTACCACAGTGTGTGAACC; primer 2: TGAACCAATGTATCCAGCACCACCTG; and bottom strand, primer 1: GGTTTTTTTAGGCTAAGATAATGGGG; primer 2: ATGGGGCTCTTTACATTTCCACAAC.
27. For the in vitro treatment of DNA, ~0.5 μg of plasmid DNA, either cut with Bam HI or at native superhelical density, was treated in 10 mM tris-Cl (pH 7.7) and 1 mM EDTA with 25 mM $KMnO_4$ for 30 s at the indicated temperatures.
28. D. A. Treco, in *Current Protocols in Molecular Biology*, F. M. Ausubel *et al.*, Eds. (Greene Publishing Associates and Wiley-Interscience, New York, 1989), pp. 13.11.1–13.11.5.
29. The *rpb1-1*–carrying yeast strain Y262 was the gift of R. Young. We also thank J. Roberts, T. O'Brien, and X. Hua for critically reading this manuscript.

1 April 1993; accepted 7 June 1993

Circularly Permuted tRNAs as Specific Photoaffinity Probes of Ribonuclease P RNA Structure

James M. Nolan, Donald H. Burke, Norman R. Pace*

Regions of *Escherichia coli* ribonuclease P (RNase P) RNA in proximity to a bound transfer RNA (tRNA) substrate were mapped by photoaffinity. A photoaffinity cross-linking reagent was introduced at specific sites in the interior of the native tRNA structure by modification of the 5′ ends of circularly permuted tRNAs (cptRNAs). The polymerase chain reaction was used for the production of cptRNA templates. After the amplification of a segment of a tandemly duplicated tRNA gene, the cptRNA gene was transcribed in vitro to produce cptRNA. Modified cptRNAs were cross-linked to RNase P RNA, and the conjugation sites in RNase P RNA were determined by primer extension. These sites occur in phylogenetically conserved structures and sequences and identify regions of the ribozyme that form part of the tRNA binding site. The use of circularly permuted molecules to position specific modifications is applicable to the study of many inter- and intramolecular interactions.

The ribonucleoprotein RNase P cleaves 5′ precursor sequences from precursor tRNAs (*1*). Bacterial RNase P RNA is catalytically active in vitro at high ionic strength in the absence of the protein component; it is a ribozyme (*2*). The model for the secondary structure of RNase P RNA is increasingly well refined, and the tertiary structure of the tRNA substrate is known (*3, 4*). To understand the structure of the catalytic complex, one must identify regions of contact between RNase P RNA and tRNA. Previously, nucleotides at or near the active site of RNase P RNA were identified with the use of a photoaffinity cross-linking reagent specifically attached at the 5′ end of mature tRNA, the site at which RNase P acts (*5*). The ability to introduce such an agent into other regions of tRNA would allow probing their interactions with the ribozyme.

Although the 5′ and 3′ termini of RNA molecules can be modified because of their unique chemical structures, specific modifications of internal sites in RNA are not easily achieved. Some internal modifications can be introduced by direct chemical RNA synthesis, but the efficiency of that process restricts its use to short molecules (*6*). A combination of chemical and enzymatic synthesis has been used to construct larger modified RNAs (*7*), but this approach is best suited for the synthesis of small amounts of material. We overcame these limitations by employing circularly permuted tRNA molecules. Circularly permuted tRNAs (cptRNAs) are tRNA structural analogs with native 5′ and 3′ ends linked by a synthetic loop and new termini in the interior of the native sequence. The choice of a particular nucleotide as the terminus of a cptRNA allows its specific modification by chemistry applicable to 5′ or 3′ ends. In general, cptRNAs can fold into biochemically active conformations (*8*).

We coupled photoagents to cptRNAs at 5′ termini that corresponded to native nucleotides 53 ($cptRNA_{53}$) or 64 ($cptRNA_{64}$) (*9*) because these nucleotides occur on the face of the tRNA molecule with which RNase P is thought to interact (*10*) (Fig. 1). To produce a template for transcription of a cptRNA, we amplified a selected portion of a tandemly duplicated gene encoding $tRNA^{Asp}$ (*11*) by polymerase chain reaction (PCR) (*12*) with primers that determined the 5′ and 3′ ends. The forward primer was a T7 RNA polymerase promoter plus the tRNA sequence selected to be the 5′ end of the cptRNA; the reverse primer determined the corresponding 3′ end. The PCR product was a cptRNA gene with a T7 promoter that could be transcribed to produce cptRNA. Transcription of PCR products in the presence of guanosine 5′-monophosphorothioate (GMPS) produced a cptRNA with a 5′-thiophosphate. This GMPS is incorporated as the first nucleotide of a transcript by T7 RNA polymerase but cannot be incorporated elsewhere in the transcript because the polymerase requires nucleoside triphosphates for chain elongation (*13*). The 5′-thiol can be specifically modified by conjugation with a photoaffinity agent for cross-linking to RNase P RNA.

We analyzed the kinetics of cleavage of cptRNAs by RNase P RNA to evaluate their suitabilities as model substrates. The ribozyme cleaves cptRNAs within the synthetic loop that connects the native 5′ and 3′ ends, so the effects of the presence of the loop and its size were tested. The cptRNAs bound well to RNase P RNA (Table 1); the Michaelis constant (K_m) of RNase P for each of the cptRNAs was no greater than threefold higher than that of the normal precursor. The catalytic rate constant (k_{cat}) for cleavage of each of the cptRNAs was five- to tenfold lower than the k_{cat} for the normal precursor. This was because the presence of the synthetic loop introduced nucleotides 3′ to the normally terminal CCA sequence. A native tRNA with nucleotides 3′ to the CCA and bipartite tRNAs with extra 3′ sequences also had a lower k_{cat} value (Table 1) (*14*). Bipartite tRNAs are formed by annealing appropriate in vitro transcripts of portions of tRNA genes (*15*). They have the same interior nick as cptRNAs but also have free termini, like normal precursor tRNAs (pre-tRNAs). The similarities of RNase P kinetics with bipartite and native tRNAs having the same CCA termini (Table 1) suggest that neither the presence of a nick in the interior of the tRNA structure nor the presence of a loop affects the binding of cptRNAs by the ribozyme. Because the differences in binding between the cptRNAs and normal pre-tRNAs to RNase P are relatively small, cptRNAs are suitable models for further study of the native reaction.

The 5′-thiolated cptRNAs produced by T7 transcription of PCR products in the presence of GMPS were coupled with azidophenacyl bromide (*5*). The ^{32}P-labeled azido-cptRNAs were incubated with RNase P RNA and irradiated at 300 nm of ultra-

J. M. Nolan and N. R. Pace, Department of Biology, Indiana University, Bloomington, IN 47405.
D. H. Burke, Department of Molecular, Cellular, and Developmental Biology, University of Colorado, Boulder, CO 80309.

*To whom correspondence should be addressed.